

Characterizations of hyaluronate-based terpolymeric hydrogel synthesized via free radical polymerization mechanism for biomedical applications



Dipankar Das^{a,b}, Thi Thu Hien Pham^{a,b}, Insup Noh^{a,b,*}

^a Department of Chemical and Biomolecular Engineering, Seoul National University of Science and Technology, Seoul 01811, Republic of Korea

^b Convergence Institute of Biomedical Engineering and Biomaterials, Seoul National University of Science and Technology, Seoul 01811, Republic of Korea

ARTICLE INFO

Keywords:

Hyaluronate
Hydrogel
Dimethylxalylglycine
Drug delivery
Tetracycline

ABSTRACT

In the present study, a novel terpolymeric hydrogel was developed using sodium hyaluronate (HA), 2-hydroxyethyl acrylate (2-HEA), and poly(ethylene glycol) diacrylate (PEGDA) via free radical polymerization for biomedical applications. To achieve elasticity, swelling ability, porous architecture and sufficient gel strength, hyaluronate was chemically modified by grafting and crosslinking methods using 2-HEA and PEGDA, respectively. The structure and compositions of the fabricated terpolymer (HA-g-p(2-HEA)-x-PEGDA) were verified by FTIR, ¹H HR-MAS-NMR, and TGA analyses. The surface morphology and cross-section of the hydrogel was detected by SEM analysis. The gel nature of terpolymer in aqueous medium at 37 °C was confirmed from swelling study, and rheological experiment. Non-cytotoxicity and biocompatibility of the HA-g-p(2-HEA)-x-PEGDA hydrogel were ascertained by *in vitro* mouse osteoblastic cells (MC3T3) proliferation, and viability studies. Hematoxylin and eosin Y, and Masson's trichrome stainings were performed to show tissue regeneration ability on the prepared hydrogel. *In vitro* release results of proangiogenic drug-dimethylxalylglycine (DMOG), and antibiotics-tetracycline (TCN) showed sustained release behaviour from the prepared hydrogel under different pHs at 37 °C. The mathematical models fitted data imply that both DMOG and TCN release follow first order kinetics, while, the release mechanism is primarily controlled by diffusion as well as erosion process. Finally, the novel biocompatible HA-g-p(2-HEA)-x-PEGDA gel, which showed sustained drugs release, and regeneration ability of extracellular matrix and collagen, could be employed in biomedical applications, especially, for the delivery of DMOG/TCN, and in tissue engineering.

1. Introduction

Hyaluronic acid is a biopolymer composed by repeating units of D-glucuronic acid and N-acetyl-D-glucosamine [1–3]. It is the major components of the skin [4] and also found in extracellular, pericellular, intracellular tissues of the body [1,3,5] and even in nuclear localization [1]. Hyaluronic acid participates in numerous biological activities, such as cell growth, migration and differentiation [6]. It is hydrophilic, biocompatible, non-immunogenic and degraded by hyaluronidases enzymes [7,8]. Moreover, the presence of hydroxyl and carboxylic acid groups in the HA moiety creates it an excellent biomaterial for chemical modifications [3,8]. These characteristics boosted the use of HA in biomaterials science ranging from tissue engineering [5,6,9–13], cosmetics [5] and drug delivery [8,14,15]. In contrast, one of the major drawbacks of single component hyaluronate is its solubility in physiological solution, which limits it to be an ideal matrix for biomedical applications such as tissue engineering and drug delivery. Hence, it is essential to modify hyaluronate by other chemical reagents to get better

efficiency for biomedical applications.

In past few years, hyaluronic acid and/or hyaluronate (HA) have been functionalized with natural polymers, synthetic polymers or nanoparticles in terms of composite materials, hydrogels or hydrogel-nanocomposites to modulate its biological and mechanical properties for better efficiency towards numerous biomedical applications [1,3,16–24]. However, taking into consideration of the biocompatibility and mechanical properties, synthetic polymers have also been widely explored in biomedical applications including tissue engineering and drug delivery [25–28]. For bone tissue engineering, the mechanical properties of bone such as elastic modulus, compressive, and tensile strength are vital [29]. These properties are highly dependent on the position of the bone and the condition of the individual. According to structure, bone tissue is classified into two types i.e. cancellous bone (trabecular) and cortical bone (lamellar) [29]. The tensile strength, compressive strength, and Young's modulus of cancellous bone are in the ranges of 10–100 MPa, 2–12 MPa, and 0.02–0.05 GPa, respectively [29]. While, the tensile strength, compressive strength, and Young's

* Corresponding author. Tel.: +822-970-6603; fax: 02-977-8317.

E-mail address: insup@seoultech.ac.kr (I. Noh).

<https://doi.org/10.1016/j.colsurfb.2018.05.059>

Received 6 April 2018; Received in revised form 19 May 2018; Accepted 26 May 2018

Available online 31 May 2018

0927-7765/ © 2018 Elsevier B.V. All rights reserved.

modulus of cortical bone are 50–150 MPa, 130–230 MPa, and 7–30 GPa, respectively [29]. Typically, HA-based hydrogels have been developed for various biomedical applications using oxidized/thiolated/acrylated/methacrylated HA, which were produced by chemical modification of –OH/–COOH group of HA using organic solvents and/or toxic chemicals [1,3,30–35]. Hydrogels are three-dimensional, hydrophilic, physically or chemically crosslinked polymer networks, having ability to absorb large amounts of water [36]. Compared to physical crosslinking, chemical crosslinking offers greater stability to HA-based hydrogels [36]. On the other hand, one of key characteristics of hydrogel is porosity through which interaction between gel, cells and the surrounding tissues occur [37–39]. Modification of the micro-architecture and the porosity of a hydrogel could always be vital concerns in biomaterial applications to deliver bioactive signals to cells growing within the developed hydrogel [37–39]. The controlled porosity endorses cellular penetration and new tissue formation within the three dimensional construction of the hydrogels [38,39]. Moreover, porosity of the hydrogel also regulates the rate swelling and drug/bioactive molecule delivery from the hydrogel [36,38,39]. Although there are several reports on hyaluronate-based hydrogel for biomedical applications [1,3,16–23]. But, keeping on mind the requisite demands of biomaterials such as sufficient strength and stability at physiological medium, higher mechanical properties, presence of interconnected pores, and excellent biocompatibility, researchers are continuously developing better and competent alternative biomaterials for biomedical applications. Our aim was synthesis of functionalized hyaluronate-based chemically crosslinked hydrogel with elastic property by avoiding the use of toxic organic solvents and reagents, which may create toxicity issue for its biological applications. For this purpose, keeping constant the structural integrity of hyaluronate, potassium persulphate was used to make hyaluronate-macroinitiator, which further initiated the polymerization of synthetic monomers followed by grafting and/or chemical crosslinking in presence of heat. 2-hydroxyethyl acrylate (2-HEA) was first grafted on the hydroxyl groups of the HA to impart elasticity [40,41]. And then graft networks were cross-linked with bi-functional poly(ethylene glycol) diacrylate (PEGDA) to tune the microstructure properties like swelling, porosity and mechanical strength [42]. There are reports on methacrylated/thiolated HA and PEGDA or HEA-based hydrogels or semi-interpenetrating network for 3-D fibroblasts spreading and migration [43], to tune cell adhesion [1], and for the release of sodium benzoate and chlorpromazine [44,45]. However, the use of three components hydrogel such as HA, 2-HEA and PEGDA towards dimethylolglycine (DMOG) and tetracycline (TCN) release, and osteoblast tissue regeneration has not been reported so far.

In the present study, HA, 2-HEA and PEGDA based terpolymeric hydrogel (HA-g-p(2-HEA)-x-PEGDA) has been synthesized by grafting and chemical crosslinking process through free radical polymerization using potassium persulfate as initiator. The amount of PEGDA has been varied to get better microstructure properties and interconnected porous network structure. Details *in vitro* cell proliferation and cytotoxicity studies using osteoblastic cells (MC3T3) have been performed by CCK, live/dead assay as well as MTT, neutral red and BrdU assays. The *in vitro* release studies of dimethylolglycine as proangiogenic drug [46,47], and tetracycline as antibiotic [48] have been carried out at pH 7.0/7.4 and 37 °C. Histological analyses such as hematoxylin and eosin Y, and Masson's trichrome staining have been carried to investigate *in vitro* tissue regeneration ability. The experimental results showed that HA-g-p(2-HEA)-x-PEGDA hydrogel contains excellent interconnected porous architecture, showed excellent biocompatibility, controlled release property of DMOG/TCN, and *in vitro* regeneration of ECM and collagen. Hence it could be used in potential biomedical applications, specifically as controlled release matrix for DMOG/TCN delivery, and tissue engineering. To our best of knowledge, this is the first report on HA, HEA and PEGDA based terpolymeric hydrogel, which is examined as a carrier of DMOG/TCN drugs, and as a matrix for

osteoblast tissue regeneration.

2. Experimental

2.1. Materials

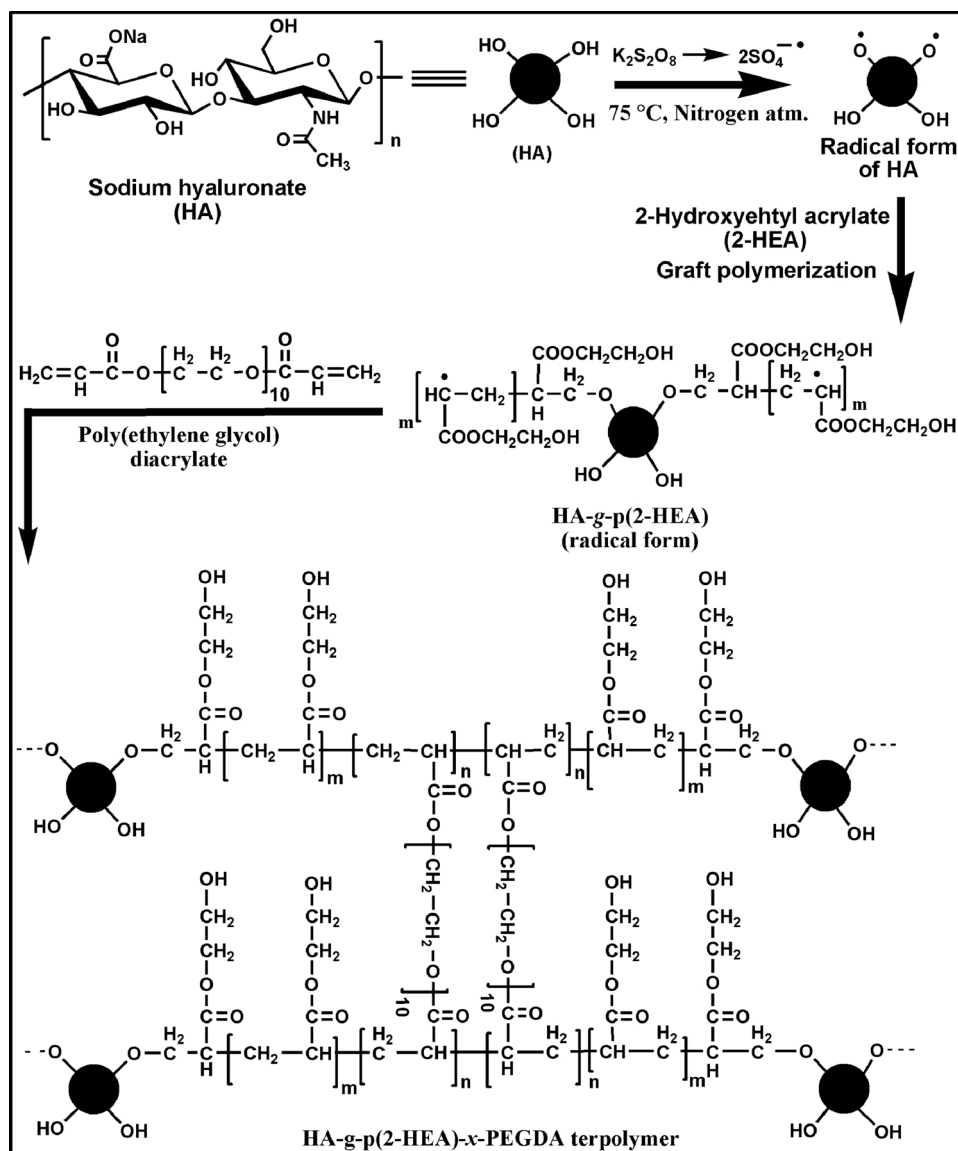
Sodium salt of hyaluronic acid (HA, Mw = 1659731 Da, PDI = 3.974) was kindly donated by Hanmi Pharm. Co. Ltd., Korea. Dimethylolglycine (DMOG, Cayman Chemical Company, USA), fetal bovine serum (FBS, Biotechnics Research, Mission Viejo, CA, USA), penicillin-streptomycin (Lonza, Seoul, Korea), cell counting kit-8 (CCK-8, Dojindo Laboratories, Kumamoto, Japan), live & dead viability/cytotoxicity kit for mammalian cells (Invitrogen, Carlsbad, CA, USA) and bromodeoxyuridine (BrdU, Roche, Germany) were purchased and used for experiment. All other chemicals such as potassium persulfate (KPS), 2-hydroxyethyl acrylate (2-HEA), poly(ethylene glycol) diacrylate (PEGDA, average MW ~575), tetracycline (TCN), α -MEM and all staining reagents were purchased from Sigma Aldrich (St. Luis, MO, USA, Germany and China). Distilled water (DW) was employed for all experiments.

2.2. Synthesis of terpolymeric gel

At first, 0.25 g HA (0.623×10^{-3} mol taking into consideration of molecular weight of one unit as shown in Scheme 1) was dissolved in 60 mL of DW in a 2-neck round bottom flask (RB) by stirring overnight at room temperature. After that, the solution was placed in digital glass oil bath (LK Lab Korea, Korea) and stirrer at 75 °C and with 400 rpm. After 2 h, nitrogen gas was purged through the RB for 30 min to make the atmosphere inert. Afterwards, 5 mL aqueous solution of KPS (2.5×10^{-3} g, 0.0092×10^{-3} mol) as an initiator was added to the HA solution. After 20 min, 2 mL of 2-HEA (17.41×10^{-3} mol) as a monomer was mixed to the solution. When the solution turned into more viscous, three different volumes such as 250 μ L (0.487×10^{-3} mol), 500 μ L (0.973×10^{-3} mol), and 750 μ L (1.460×10^{-3} mol) of PEGDA as a crosslinker were separately added for the synthesis of three grades terpolymeric crosslinked hydrogel. After addition of PEGDA, the reaction was processed for another 3 h. Lastly, the product was dialyzed in distilled water at 25 °C for 48 h. Then the purified samples were dried at lyophilizer at –56 °C for 7 days, called as dry HA-g-p(2-HEA)-x-PEGDA sample.

2.3. Characterizations

Molecular weight of the hyaluronic acid sodium salt (HA, Hanmi Pharm. Co. Ltd., Korea) was determined on a gel permeation chromatography (Model: Tosoh EcoSEC HLC-8320 GPC) equipped with $2 \times$ Tskgel GMPW \times 1 + Tskgel G2500PW \times 1 and RI detector at Korea Polymer Testing and Research Institute (KOPTRI, Seoul, Korea). FTIR spectra were recorded using ATR-FTIR spectrometer (Model: Travel IR, Smiths Detection, USA). The wavelength range of spectra was 650–4000 cm^{-1} . The ^1H NMR spectra were executed with nuclear magnetic resonance (NMR) spectrometer (Model: DD2 700, Agilent Technologies-Korea, USA). The HR-MAS NMR spectrum (proton) of HA-g-p(2-HEA)-x-PEGDA gel was recorded in Korea Basic Science Institute (Seoul, Korea) using AVIII 700 MHz NMR spectrometer (Bruker Instruments, Inc., Germany) using D₂O as solvent. The thermogravimetric analyses were performed using thermogravimetric analyser (TGA, Model: DTG-60, Shimadzu, Japan) at nitrogen atmosphere, where scan rate was 5 °C/min. The surface and cross-section morphology of samples were observed by SEM (Model: SEM, TESCAN VEGA3, Tescan Korea). The pore size was measured by ImageJ software, and porosity was determined using liquid displacement method using hexane as solvent [49]. The method of porosity determination is discussed in detail in the Supporting information.



Scheme 1. Probable mechanism for the formation of terpolymeric HA-g-p(2-HEA)-x-PEGDA gel.

2.4. Swelling study

The % swelling of the three grades of dried HA-g-p(2-HEA)-x-PEGDA samples were measured gravimetrically at pH 7.0/7.4, and $37\text{ }^\circ\text{C}$. The swelling study is depicted in detail in the Supporting information.

2.5. Rheological analysis

Rheological analysis of dialyzed HA-g-p(2-HEA)-x-PEGDA gel was performed in Korea Polymer Testing and Research Institute (Koptri; Seoul, Korea) by rotational rheometer (TA Instrument Ltd., DHR-1, Germany) at the temperature of $37\text{ }^\circ\text{C}$. The analysis was carried out using 25 mm parallel plate with measuring gap of 1 mm. Frequency sweep measurement was executed with the range of 0.1–10 Hz. For stress sweep measurement, oscillation stress range was 1–1000 Pa with a constant frequency of 1 Hz. Shear viscosity of the gel samples was measured between the shear rate range of 0.1–1300/s.

2.6. In vitro cell study on HA-g-p(2-HEA)-x-PEGDA gel

2.6.1. Osteoblast cell (MC3T3) behaviours on the surface of HA-g-p(2-HEA)-x-PEGDA gel film

In vitro osteoblast cell (MC3T3) proliferation study was performed on the surface of HA-g-p(2-HEA)-x-PEGDA gel film to confirm the biocompatibility of the hydrogel. The degrees of cell proliferation were evaluated by CCK-8 assay by following our previous protocols [50]. The images of MC3T3 cells on hydrogel film were captured using live and dead viability/cytotoxicity kit by a fluorescence microscope (Leica DMLB, Wetzlar, Germany) as described in the literatures [50,51]. The details procedure of this study is described in Supporting information.

2.6.2. Evaluation of cytotoxicity of HA-g-p(2-HEA)-x-PEGDA gel

The *in vitro* toxicity of the HA-g-p(2-HEA)-x-PEGDA gel was determined against cell organs like mitochondria, lysosome and DNA by MTT, Neutral Red and BrdU assays, respectively [50,51]. The details process is described in Supporting information.

2.7. *In vitro* drug release study

2.7.1. Incorporation of dimethyloxalylglycine (DMOG) and tetracycline (TCN) in HA-g-p(2-HEA)-x-PEGDA gel and *in vitro* release study

Two different amounts (14 and 28 μmol) of DMOG and TCN were incorporated separately in 0.5 mL of HA-g-p(2-HEA)-x-PEGDA gel (optimized grade) through mixing in a 48 well plate by a spatula until the drugs were completely dissolved. The height and diameter of the drugs loaded gels were 7 mm and 10 mm, respectively. Then, the loaded gels were dried in a lyophilizer at -60°C for 72 h. After drying, the average diameter (2r) and height (h) of the loaded cylindrical shaped gels were 6 ± 1 mm, 6 ± 1 mm, respectively. The dried weights of the 14 and 28 μmol DMOG containing gels were 27.8 ± 0.2 mg, and 30.3 ± 0.2 mg, respectively. Whereas, the dried weights of the 14 and 28 μmol TCN containing gels were 31.6 ± 0.2 mg, and 37.9 ± 0.2 mg, respectively.

The *in vitro* DMOG and TCN release studies of dried drug-loaded gels were performed at pH 7.0/7.4, and 37°C . To observe the effect of pH, and impact of swelling on drugs release behaviour, two different pHs (7.0 and 7.4) were chosen. Besides, to detect the release nature at the same pH (7.4) where *in vitro* osteoblast regeneration study was performed, the physiological pH i.e. pH 7.4 was selected in this study. Briefly, the drugs loaded gels were put in flasks containing 100 mL of buffer media (pH 7.0 and 7.4) at 37°C . After 1, 3, 6, 12, 24, 48, 72 and 96 h, aliquots were taken out from flasks and absorbance were measured by UV-vis spectrophotometer (Model: BioMATE 3, Thermo Scientific, Madison, USA). After each measurement, buffer solutions were replaced by new buffer solutions. The% DMOG and TCN release were calculated on the basis of standard drugs solutions. For each samples, experiments were performed in triplicate.

2.7.2. Evaluation of DMOG and TCN release kinetics and mechanism

The *in vitro* DMOG and TCN release data were fitted in zero order and first order kinetics models [36] to find out the kinetics of the drugs release from the HA-g-p(2-HEA)-x-PEGDA gel (optimized grade). While, the mechanism of the DMOG/TCN release was evaluated by fitting the data in Higuchi [52], Peppas-Sahlin [53], and Kopcha models [52]. The release kinetics and mechanism determination models are discussed in detail in the Supporting information.

2.8. Histological analyses

The histological analyses of thin films of 100 μL of dried HA-g-p(2-HEA)-x-PEGDA 2 gel ($d = 1$ cm) containing MC3T3 cells were performed by hematoxylin and eosin Y (H&E) and masson's trichrome (MT) stainings. The purposes of these staining were to observe the formation of ECM, collagen, and prominent nucleus of MC3T3 cells on the HA-g-p(2-HEA)-PEGDA gel film so that it could be ascertained that the synthesized gel could be used in tissue engineering applications. The procedure of histological analyses is discussed in detail in the Supporting information.

2.9. Statistical analysis

All data were stated as mean \pm standard deviation. Statistical significance was evaluated with one-way and multi-way ANOVA by using the SPSS 18.0 program (ver. 18.0, SPSS Inc., Chicago, IL, USA). The comparisons between two groups were performed by *t*-test and significant difference has been reported when $p < 0.05$ [50].

3. Results and discussions

3.1. Synthesis of terpolymeric HA-g-p(2-HEA)-x-PEGDA gel

Three grades of terpolymeric gel have been synthesized using HA (0.25 g, 0.623×10^{-3} mol) as main biopolymer, 2-HEA (2 mL,

17.41×10^{-3} mol) as monomer and KPS (2.5×10^{-3} g, 0.0092×10^{-3} mol) as initiator. The amount of crosslinker (PEGDA) was varied using 250 μL (0.487×10^{-3} mol), 500 μL (0.973×10^{-3} mol), and 750 μL (1.46×10^{-3} mol) to get gel with different porous architectures. It is assumed that in presence of heat, one molecule KPS forms two sulphate anion radicals ($\text{SO}_4^{2-\cdot}$) in the inert atmosphere (Scheme 1). These sulphate anion radicals abstract hydroxyl protons from HA and generate radicals on HA. Compare to hyaluronate, ~ 1.47 mol% initiator was used. Thus, it is anticipated that ~ 2.94 mol% sulphate anion radicals may have been generated in the reaction medium and formed HA radicals. When 2-HEA was added, those% HA-radicals (~ 2.94 mol%) reacted with 2-HEA molecules. At this time, the solution started to change its viscosity, which suggested grafting of 2-HEA onto the HA followed by polymerization and formation of radical species of HA-g-p(2-HEA) (Scheme 1). Predefined amounts of PEGDA were added to crosslink the graft copolymers. It is noticed that the moles of PEGDA are higher in all three reactions than those of expected generated radicals on the graft products (as mole of KPS is lower than PEGDA). Consequently, it is hypothesized that while PEGDA was added: (i) at first, the reactive radicals of graft products attack on PEGDA, and once all the graft radical sites were attached with the PEGDA (assuming inter-crosslinking), after that, (ii) the rest of the PEGDA molecules reacted with each other and polymerized (Scheme 1). Hence, it is predictable that PEGDA not only crosslinked two graft polymers but also self-polymerized in the reaction condition. The probable mechanism is represented in Scheme 1. Three grades of gels have been designated as HA-g-p(2-HEA)-x-PEGDA 1, HA-g-p(2-HEA)-x-PEGDA 2 and HA-g-p(2-HEA)-x-PEGDA 3 on the basis of used 250 μL , 500 μL , and 750 μL of PEGDA amount (digital images in Fig. S1, Supporting information). The grade, HA-g-p(2-HEA)-x-PEGDA 2 is selected as optimized grade for details characterizations and application because of its well defined porous network which is depicted in scanning electron microscopy (SEM) analysis section.

3.2. Characterization

Fig. S2 (Supporting information) designates the GPC study result of sodium hyaluronate (HA) employed for the development of terpolymeric hydrogel. It is detected that the peak top for the elution time was 18.567 min (Fig. S2a, Supporting information). The number average (M_n) and weight average (M_w) molecular weights were 414680 and 1659731 Da, while PDI value was 3.974 (Fig. S2b, Supporting information).

Fig. S3 (Supporting information) represents FTIR spectra of sodium HA, 2-HEA, PEGDA, and dried HA-g-p(2-HEA)-x-PEGDA samples. In the FTIR spectrum of HA, the peaks at 3301 and 2902 cm^{-1} are responsible for the stretching vibrations of O–H/N–H bond and C–H bond [54]. The peaks at 1609 and 1406 cm^{-1} are due to the stretching vibrations of C=O and C–O bonds of –COO– group [54], while the peaks for C–O–C asymmetric and symmetric stretching frequencies appeared at 1147 and 1038 cm^{-1} (Fig. S3a, Supporting information). In the FTIR spectrum of 2-HEA, the peaks at 3429, 2953, 2885, 1717, and 1632 cm^{-1} are due to the stretching frequencies of O–H, C–H, C=O, and C=C bonds, respectively (Fig. S3b, Supporting information). The peaks at 1408, 1276 and 1189 cm^{-1} are owing to C–H bending, C–O, and C–O–H stretching frequencies, respectively (Fig. S3b, Supporting information). In the FTIR spectrum, PEGDA demonstrates peaks at 2870, 1723, 1633, 1192, and 1101 cm^{-1} which are responsible for the stretching frequencies of C–H, C=O, C=C, C–O and C–O–C bonds, respectively (Fig. S3c, Supporting information). In the FTIR spectrum, HA-g-p(2-HEA)-x-PEGDA polymer shows peaks at 3415, 2938, and 1723 cm^{-1} are due to the stretching frequencies of O–H/N–H, C–H, and C=O bonds, respectively (Fig. S3d, Supporting information). The peaks at 1448, 1242, 1162, and 1074 cm^{-1} are because of C–H bending, and stretching frequencies of C–O, C–O–H, and C–O–C bonds, respectively (Fig. S3d, Supporting information). The new peaks

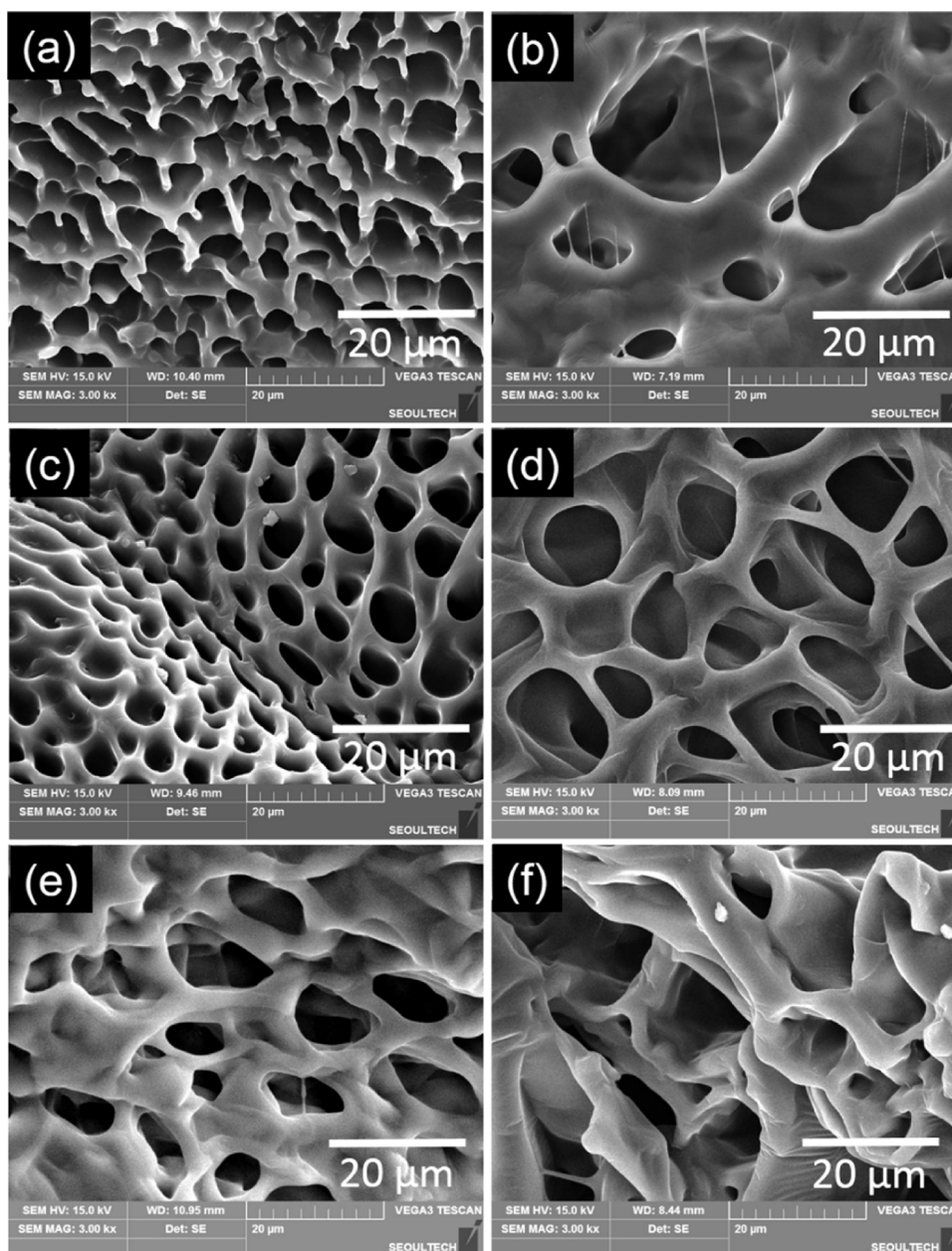


Fig. 2. SEM results: surface morphologies (a, c, e), and cross-section (b, d, f) of lyophilized HA-g-p(2-HEA)-x-PEGDA 1, 2, 3 gels, respectively (Magnification = 3 kx).

the second gel (HA-g-p(2-HEA)-x-PEGDA 2) demonstrated well-defined porous architecture (Fig. 2c), which is may be due to homogeneous and adequate crosslinking. The ImageJ software results showed that the average surface pore size of HA-g-p(2-HEA)-x-PEGDA 1, HA-g-p(2-HEA)-x-PEGDA 2, HA-g-p(2-HEA)-x-PEGDA 3 was $5.2 \pm 1.1 \mu\text{m}$, $4.7 \pm 0.9 \mu\text{m}$, and $5.6 \pm 1.1 \mu\text{m}$, respectively. The HA-g-p(2-HEA)-x-PEGDA 1 gel showed porous network (Fig. 2a), but porosity is higher in HA-g-p(2-HEA)-x-PEGDA 2 gel ($53.4 \pm 0.5\%$) than that in HA-g-p(2-HEA)-x-PEGDA 3, porosity ($39.3 \pm 0.2\%$) again decreased, which is owing to the higher crosslinking density because of the employment of highest amount of crosslinker (PEGDA). The cross-section images signify that pores are interconnected to each other (Fig. 2b, d, f).

HA showed three weight loss zones in TGA analysis [56]. The zone below 100°C is because of moisture evaporation, and the zones $150\text{--}260^\circ\text{C}$, $260\text{--}440^\circ\text{C}$, and $450\text{--}600^\circ\text{C}$ are due to the complete breakdown of polysaccharide backbone and evaporation CO_2 [56]. In the TGA plot of HA-g-p(2-HEA)-x-PEGDA 2 gel (Fig. 3a), the first

weight loss region (below 100°C) is because of the evaporation of moisture, the second zone ($187\text{--}311^\circ\text{C}$) is due to breakdown of HA unit, and the wide weight loss region ($311\text{--}440^\circ\text{C}$) is for the breakdown of both 2-HEA and PEGDA unit.

3.3. Swelling study

Fig. 3b–c represents swelling test results of three grades of HA-g-p(2-HEA)-x-PEGDA gel at pH 7.0, pH 7.4 and 37°C . From Fig. 3b–c, it is obvious that HA-g-p(2-HEA)-x-PEGDA gel reached in an equilibrium state of swelling at about 12 h in both media, which confirmed the hydrogel formation behaviour of the cross-linked polymer. Among three grades, HA-g-p(2-HEA)-x-PEGDA 3 showed the lowest% equilibrium swelling ratio ($457 \pm 22\%$ at pH 7, and $752 \pm 18\%$ at pH 7.4). This result may be due to the higher% crosslinking in HA-g-p(2-HEA)-x-PEGDA 3, and presence of the lower amount of pores into the gel network (Fig. 2) compared to the other two grade gels. Among first two grades, HA-g-p(2-HEA)-x-PEGDA 2 showed lower% equilibrium

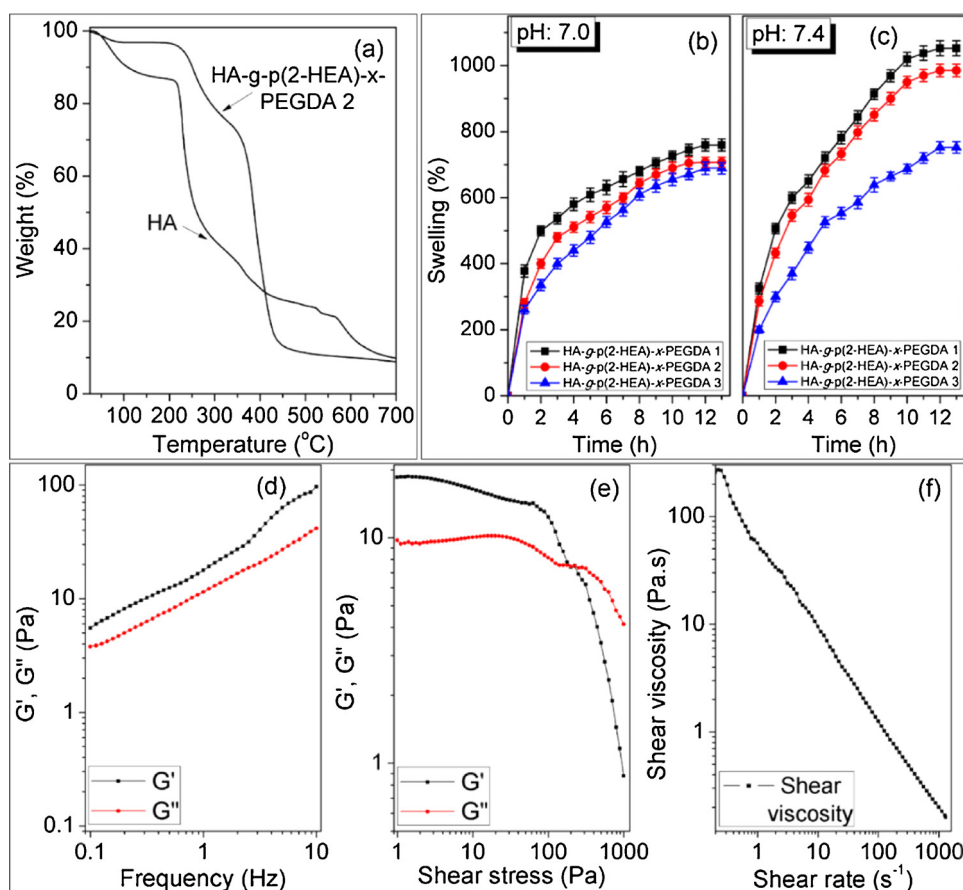


Fig. 3. (a) TGA plots of HA, and dried HA-g-p(2-HEA)-x-PEGDA 2 gel, and swelling (%) vs. time (h) plot of three grades of gel at (b) pH: 7.0, and (c) pH: 7.4 and 37 °C (Results are represented as average \pm SD, $n = 3$), and (d-f) rheology study results of dialyzed HA-g-p(2-HEA)-x-PEGDA gel (optimized grade) at 37 °C.

swelling ratio ($509 \pm 25\%$ at pH 7, and $985 \pm 19\%$ at pH 7.4) than that of HA-g-p(2-HEA)-x-PEGDA 1 ($526 \pm 26\%$ at pH 7, and $1053 \pm 23\%$ at pH 7.4). Although, no significant difference is observed from the surface morphology of these two gels, while, cross-section images display bigger sizes of pores in HA-g-p(2-HEA)-x-PEGDA 1 than that of HA-g-p(2-HEA)-x-PEGDA 2 (Fig. 2), which may be one of the causes for higher% swelling of HA-g-p(2-HEA)-x-PEGDA 1. Besides, the amount of crosslinker (PEGDA) is higher in grade 2 gel than that of grade 1 gel. Moreover, all grades of HA-g-p(2-HEA)-x-PEGDA gel exhibited higher% equilibrium swelling ratio at pH 7.4 than pH 7.0 (Fig. 3b–c). This is because of the high charge density (due to presence of negative carboxylate ions) over the gels at pH 7.4 than that of pH 7.0, which increased the hydrophilicity of the gels, resulting in higher% equilibrium swelling ratio at pH 7.4.

3.4. Rheology study

The rheological characteristics of the dialysed HA-g-p(2-HEA)-x-PEGDA gel has been performed at 37 °C. From the frequency sweep experiment (Fig. 3d), it is apparent that elastic modulus (G') is higher than that of viscous modulus (G'') and both moduli increased with increase of frequency, which signify the material is a gel with elasticity [36]. From amplitude sweep study (Fig. 3e), it is obvious that elastic modulus (G') is higher than that of viscous modulus (G''). It has been seen that after the shear stress value of 63 Pa, elastic modulus value starts to decreased sharply. Whereas, at the shear stress of ~ 203 Pa, the viscous modulus of the gel overcomes the elastic modulus which indicates flow nature of the gel at the experimental condition and the point is known as yield stress of the HA-g-p(2-HEA)-x-PEGDA gel. Before reaching that point, the gel strength was measured as 1.03 ($G'/$

$G'' = 7.79/7.56$). Again, from Fig. 3f, it is noticed that the shear viscosity of the HA-g-p(2-HEA)-x-PEGDA gel continuously decreased with increasing of shear rate. This characteristic indicates non-Newtonian shear thinning behaviour of the gel. The nature of gel and mechanical property of HA-g-p(2-HEA)-x-PEGDA gel implies that it could be used as a filler with bioactive molecule release ability for small and irregular defects in cancellous bone.

3.5. *In vitro* cell study on HA-g-p(2-HEA)-x-PEGDA gel

3.5.1. Osteoblast cell (MC3T3) culture and proliferation studies on the surface of HA-g-p(2-HEA)-x-PEGDA gel film

Fig. 4 depicts the *in vitro* MC3T3 cell culture study results of HA-g-p(2-HEA)-x-PEGDA gel film (optimized grade). From Fig. 4a, it is obvious that with increase of time (1, 3, 5 and 7 days), the optical densities are increased on both control (tissue culture plate) and HA-g-p(2-HEA)-x-PEGDA gel film, which signify that the MC3T3 cells were progressively grew and proliferated on both control and hydrogel film.

However, Fig. 4b suggests that the rate of MC3T3 cells proliferation was higher on gel film than that of control. This study implies that HA-g-p(2-HEA)-x-PEGDA gel film provided cordial substrate for cell growth and proliferation. Fig. 4d–g showed *in vitro* cellular attachment on the surface of HA-g-p(2-HEA)-x-PEGDA gel film, detected by the ethidium homodimer-1 and calcein AM assay at 1, 3, 5 and 7 days. The gradual increase in MC3T3 cell population after 1, 3, 5 and 7 day cultures established that the cells with low population exhibit no desired connection with each other at day 1 and 3 (Fig. 4d–e). While, at day 5 and 7, the cellular populations were more distinct on the surface of the gel film (Fig. 4f–g). The cell-cell contacts were observed, and formation of excellent three dimensional array of MC3T3 cells was noticed. The cell

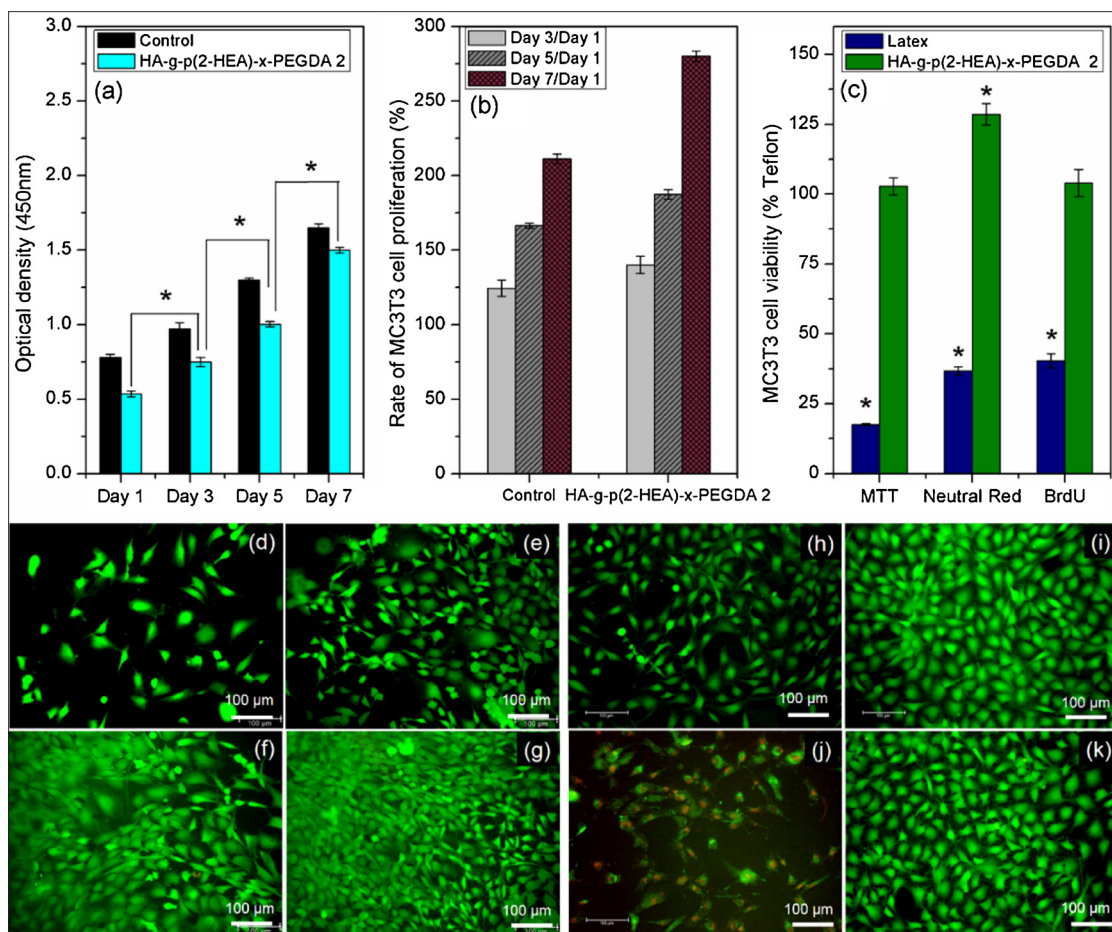


Fig. 4. (a) Optical density of MC3T3 cells after 1, 3, 5 and 7 days on TCP (control) and gel films, (b) rate of cell proliferation on the surface of the HA-g-p(2-HEA)-x-PEGDA gel film, (c) cytotoxicity results of gel films, (d–g) MC3T3 cells images by live and dead assay on the surface of the gel film using ethidium homodimer-1 and calcein AM assay after 1, 3, 5 and 7 days, respectively, and (h) MC3T3 cells images before extract addition, and (i–k) after the addition of extract from teflon as a positive control, latex as a negative control and gel films, respectively. (Results are represented as average \pm SD, $n = 3$).

growth features reveal that the HA-g-p(2-HEA)-x-PEGDA gel provided an excellent matrix for osteoblast cell growth and proliferation without cytotoxicity, and could be a suitable biomaterial for bone tissue engineering. Although, the cells proliferation is higher in the hydrogel film by the effects of gel property itself such as gel network and chemical composition, other factors such as biophysical properties, especially the nanostructures, may be important in controlling of the cell behaviours. Other research groups reported that the nanotopography of the gel matrix can act as a potent modulator of cell behaviours in tissue regeneration [57–59].

3.5.2. Evaluation of cytotoxicity of HA-g-p(2-HEA)-x-PEGDA gel

In vitro viability of the HA-g-p(2-HEA)-x-PEGDA gel (optimized grade) has been detected by measuring cytotoxicity against mitochondria, lysosome and DNA of MC3T3 cells using MTT, Neutral Red and BrdU assays, respectively. In this study, the extract solution of gel film has been used to compare viability with those of teflon and latex extracts. The viability value of teflon (positive control) is considered as 100%. Latex is used as negative control. From Fig. 4c, it is evident that % cell viability of gel is higher than those of teflon and latex (Fig. 4c). The gel showed $103 \pm 3\%$, $128 \pm 4\%$, and $104 \pm 5\%$ cell viability (Fig. 4c). Whereas, viability is significantly decreased in latex (Fig. 4c). The effect of three extracts (teflon, latex and gel films) on MC3T3 cells viability was further supported by the fluorescence images of MC3T3 cells (Fig. 4h–k). Cells were grown well in presence of extracts of teflon (Fig. 4i) and gel films (Fig. 4k), no dead cells were found. While, many dead cells are perceived for latex extract (Fig. 4j). This study confirmed

that HA-g-p(2-HEA)-x-PEGDA gel did not release any toxic compounds, i.e. indicating a non-toxic and biocompatible gel, and could be a suitable choice for biomedical applications.

3.6. *In vitro* release of DMOG and TCN from HA-g-p(2-HEA)-x-PEGDA gel

Fig. 5 represents *in vitro* release profiles of DMOG and TCN from HA-g-p(2-HEA)-x-PEGDA gel (optimized grade) at pH 7.0/7.4 and 37 °C. DMOG is a low molecular drug and a cell penetrant oxoglutarate equivalent which can prevent prolyl hydroxylase (PHD) enzymes [60]. Consequently, it controls the stability of hypoxia inducible factor (HIF)-1 α in cells and induces downstream gene expression [60]. HIF-1 α is a vital mediator of the adaptive cells response to hypoxia that has a significant role in angiogenesis-osteogenesis coupling during bone regeneration [60]. Besides, DMOG can increase the bone healing capability of adipose-derived stem cells (ASCs) by improving osteogenic differentiation and angiogenic potential [60]. It can also increase the angiogenic activity of bone marrow stromal cells (BMSCs) by triggering the expression of HIF-1 α in cells, and thus advance the angiogenesis of the tissue-engineered bone [60]. On the other hand, TCN is an antibiotic which affects inflammation, immunomodulation, cell proliferation, and angiogenesis [61]. TCN prevents activities of matrix metalloproteinases (MMPs), which proteolytically breakdown several constituents of the extracellular matrix (ECM) into collagenases and gelatinases [61]. TCN can inhibit both collagenases and gelatinases [61]. Generally, drugs are released from a hydrophilic polymer matrix through four ways [36,53]: (i) dissolution process (surface drug), (ii)

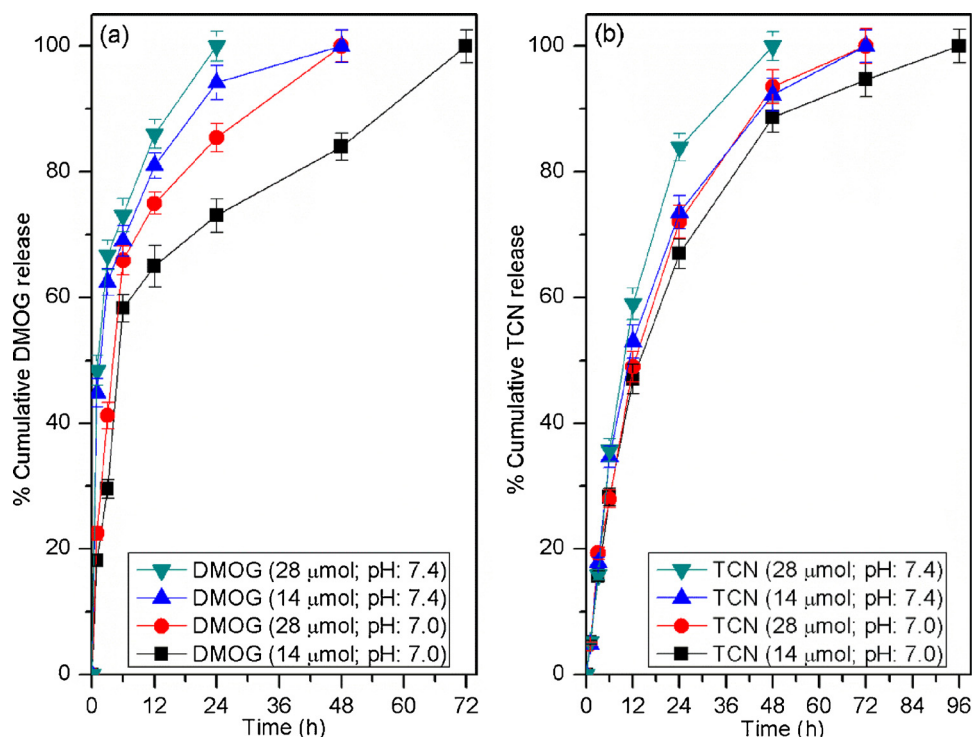


Fig. 5. *In vitro* release profiles of (a) DMOG, and (b) TCN from the loaded HA-g-p(2-HEA)-x-PEGDA gel (optimized grade) at pH 7.0/7.4 and 37 °C (results are represented as average \pm SD, n = 3).

diffusion process, (iii) relaxation of the matrix, (iv) erosion of the matrix. Here, two different amounts (14 μ mol and 28 μ mol) of DMOG and TCN were incorporated into the gels and *in vitro* release study was performed at pH 7.0 and 7.4. It is observed that release rates of both DMOG and TCN are quicker at pH 7.4 than that at pH 7.0 (Fig. 5a–b), which is because of the higher rate of swelling of the gel at pH 7.4 [36].

At pH 7.4, gel network possesses negative charge (owing to carboxylate ions of HA) that accelerates to absorb large number of water molecules, ensuing higher rate of swelling. Between two doses of drug (DMOG/TCN), formulations bearing high dose (28 μ mol) showed higher rates of DMOG/TCN release (Fig. 5a–b). Principally, high dose of DMOG/TCN reduces the percentage of gel content in the formulation. Therefore, the gel layer through which DMOG/TCN freely diffuse became weaker, resulting higher rate of DMOG/TCN release [62]. In addition, for high dose formulation, the higher rates of DMOG/TCN release are also affected by the quick release of drugs at the initial period, where most of the drugs may release from the surface of the gel [62]. At the initial time, when the formulation makes contact with the dissolution medium, the surface drugs molecules rapidly release [62,63]. Furthermore, from Fig. 5a–b, it is also noticed that DMOG executes quicker release rate than that of TCN in both media. This phenomenon is owing to the difference of molecular weight between DMOG (MW- 175.14 g/mol), and TCN (MW- 444.43 g/mol). Generally, a low molecular weight drug has shorter mean dissolution time than that of a high molecular weight drug [62,64]. Consequently, the low molecular weight drug (DMOG) diffuses through the gel layer more readily than that of the high molecular weight drug (TCN). From the drug release results, it is also obvious that the DMOG and TCN loaded hydrogel could assist the pre-angiogenesis-osteogenesis process. However, the \sim 100% release of DMOG and TCN drugs between 24 and 96 h (depending on the nature and amount of dose) suggests that to advance angiogenesis/osteogenesis for bone regeneration, both drugs should be additionally added during the experiment after regular times of interval, as an example, by controlling crosslinking density of gel networks.

3.6.1. Drug release kinetics and mechanism

From the coefficient of determination (R^2) value, it is observed that the release data is well fitted (higher R^2 value, Table S1-S2, Supporting information) with first order kinetics model than that of zero order kinetic model. The results imply that both drugs (DMOG and TCN) follows first order kinetics. While, from the release mechanism determination models (Higuchi, Peppas-Sahlin, and Kopcha), it is obvious that the release data are well fitted with Peppas-Sahlin model, where the relaxational contribution (K_2) is negligible compared to diffusion contribution (K_1) (Table S1-S2, Supporting information). Besides, the diffusional exponent (A) is also higher than the erosional exponent (B) derived from Kopcha model (Table S1-S2, Supporting information). Hence, from both Peppas-Sahlin, and Kopcha models, it is obvious that both DMOG and TCN release from HA-g-p(2-HEA)-x-PEGDA gel is mostly controlled by diffusion process, however, erosion of matrix also has lower contribution in release [36,52].

3.7. Histological analyses: hematoxylin and eosin Y (H&E) staining, and Masson's trichrome (MT) staining

Fig. 6 depicts the results of H&E and MT staining of HA-g-p(2-HEA)-x-PEGDA gel film, which cultured with MC3T3 cells for 14, 21, and 28 days. From H & E staining image (Fig. 6a), it is observed that on day 14, cells were grown and spread well on the gel film, blue-coloured nuclei are obvious. However, collagen in ECM (pink coloured) is limited. On day 21, it is apparent that the cells are connected with each other, while ECM is well developed (Fig. 6b). On day 28, well developed pink-coloured ECM is clearly visible and it is spread throughout the film, thereby cells are connected to each other, which indicate tissue regeneration on the HA-g-p(2-HEA)-x-PEGDA gel film (Fig. 6c). From MT staining results, brown-coloured prominent nuclei of the MC3T3 cells and their collagen formation are observed on day 21 (Fig. 6e) compared to those at day 14 (Fig. 6d). On day 28, it is obvious that blue-coloured collagen is formed in all over the ECM (Fig. 6f), which confirmed that HA-g-p(2-HEA)-x-PEGDA gel film provided a suitable matrix for tissue regeneration.

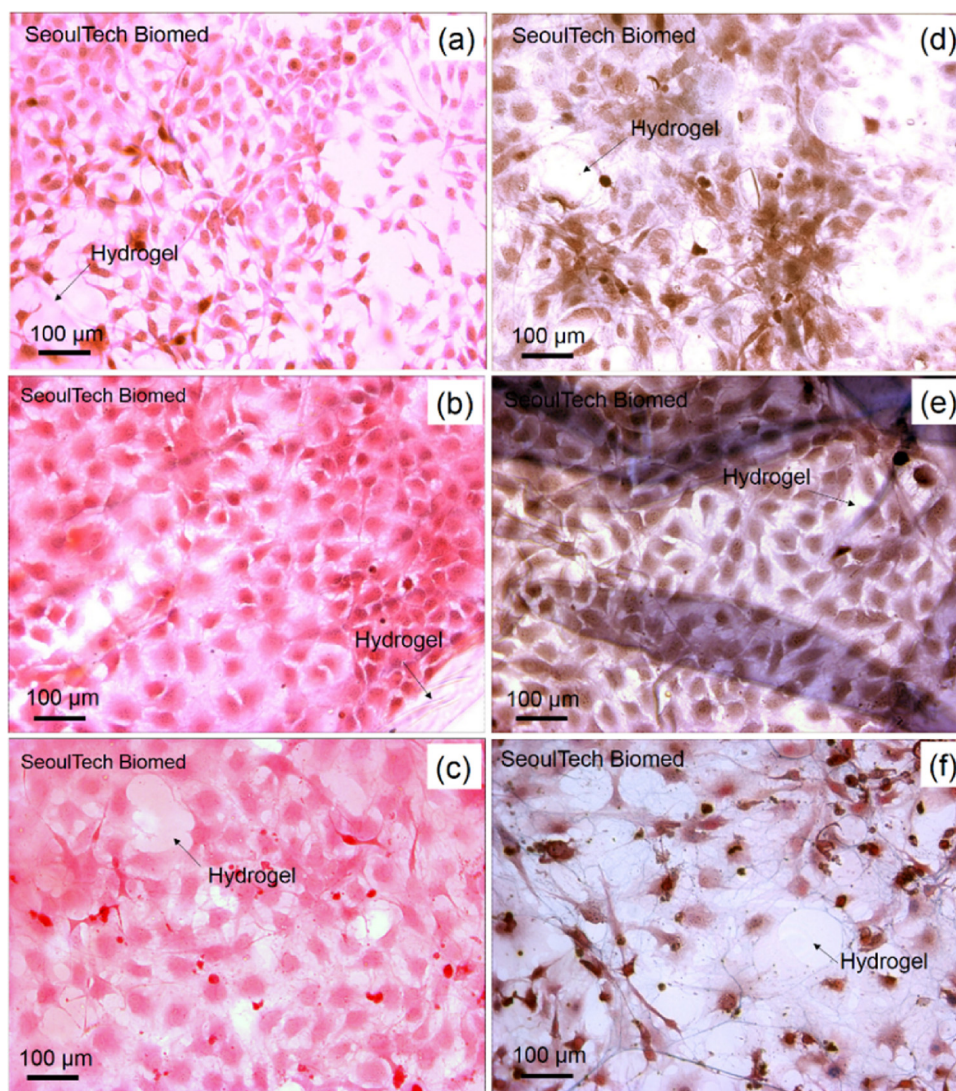


Fig. 6. Staining results of H&E (a, b, c), and MT (d, e, f) of HA-g-p(2-HEA)-x-PEGDA gel film after *in vitro* MC3T3 cells cultured for 14, 21 and 28 days, respectively.

4. Conclusions

The HA-g-p(2-HEA)-x-PEGDA terpolymeric gel has been successfully synthesized through free radical polymerization using HA, 2-HEA and PEGDA. The structure and compositions of gel has been confirmed by FTIR, $^1\text{H-NMR}$, and TGA analyses. The achievement of equilibrium swelling ratio, and higher value of elastic modulus (G') confirmed the gel nature of terpolymeric system in aqueous medium at 37°C . By grafting HEA molecule and changing the amount of PEGDA as crosslinker, gel strength, microstructure and porosity of the HA-g-p(2-HEA)-x-PEGDA gel changed significantly. The moderate amount of PEGDA (500 μL) in this study generated a well-defined interconnected porous network, which is suitable for both drug delivery and tissue engineering applications. The evaluation of the potential applicability of HA-g-p(2-HEA)-x-PEGDA gel as biomaterial has been performed by observing the results of cell compatibility, *in vitro* tissue regeneration capability and release behaviours of bioactive molecules such as DMOG and TCN. Release profiles of DMOG and TCN demonstrated pH-dependent sustained release up to 3-4 days, where, release rate was quicker at pH 7.4 than that of pH 7.0. The *in vitro* MC3T3 cell viability and cytotoxicity results using CCK, live/dead, MTT, MTT, BrdU, and neutral red assays confirmed that the HA-g-p(2-HEA)-x-PEGDA gel is biocompatible and non-cytotoxic. The results indicate that the interconnected porous architecture and 3D network of the HA-g-p(2-HEA)-x-

PEGDA gel endorsed excellent osteoblastic cell adhesion, proliferation, and viability. The H&E and Masson's trichrome staining results displayed that ECM including collagen were formed and well-developed after 3 weeks. Overall, the novel, porous, biocompatible, HA-g-p(2-HEA)-x-PEGDA gel could be used in biomedical applications, especially, for the delivery of DMOG/TCN, and as a filler for small defect in bone tissue engineering.

Acknowledgement

Authors also sincerely acknowledge the financial support of National Research Foundation of Korea (NRF) Grant (2015R1A2A1A10054592).

Appendix A. Supplementary data

Supplementary data associated with this article can be found, in the online version, at <https://doi.org/10.1016/j.colsurfb.2018.05.059>.

References

- [1] S. Ouasti, R. Donno, F. Cellesi, M.J. Sherratt, G. Terenghi, N. Tirelli, Network connectivity, mechanical properties and cell adhesion for hyaluronic acid/PEG hydrogels, *Biomaterials* 32 (2011) 6456–6470.
- [2] F. Roig, M. Blanzat, C. Solans, J. Esquena, M.J. Garcia-Celma, Hyaluronan based

- materials with cationic sugar-derived surfactants as drug delivery systems, *Colloids Surf. B, Biointerfaces* 164 (2018) 218–223.
- [3] E. Larraneta, M. Henry, N.J. Irwin, J. Trotter, A.A. Perminova, R.F. Donnelly, Synthesis and characterization of hyaluronic acid hydrogels crosslinked using a solvent-free process for potential biomedical applications, *Carbohydr. Polym.* 181 (2018) 1194–1205.
- [4] A. Mero, M. Campisi, Hyaluronic acid bioconjugates for the delivery of bioactive molecules, *Polymers-Basel* 6 (2014) 346–369.
- [5] M.N. Collins, C. Birkinshaw, Hyaluronic acid based scaffolds for tissue engineering—a review, *Carbohydr. Polym.* 92 (2013) 1262–1279.
- [6] M. Hemshekhar, R.M. Thushara, S. Chandranayaka, L.S. Sherman, K. Kemparaju, K.S. Girish, Emerging roles of hyaluronic acid bioscaffolds in tissue engineering and regenerative medicine, *Int. J. Biol. Macromol.* 86 (2016) 917–928.
- [7] C.B. Highley, G.D. Prestwich, J.A. Burdick, Recent advances in hyaluronic acid hydrogels for biomedical applications, *Curr. Opin. Biotechnol.* 40 (2016) 35–40.
- [8] G. Tripodo, A. Trapani, M.L. Torre, G. Giammona, G. Trapani, D. Mandracchia, Hyaluronic acid and its derivatives in drug delivery and imaging: recent advances and challenges, *Eur. J. Pharm. Biopharm.* 97 (2015) 400–416.
- [9] F. Yu, X.D. Cao, Y.L. Li, L. Zeng, B. Yuan, X.F. Chen, An injectable hyaluronic acid/PEG hydrogel for cartilage tissue engineering formed by integrating enzymatic crosslinking and Diels-Alder click chemistry, *Polym. Chem.-UK* 5 (2014) 1082–1090.
- [10] J. Yeom, B.W. Hwang, D.J. Yang, H.I. Shin, S.K. Hahn, Effect of osteoconductive hyaluronate hydrogels on calvarial bone regeneration, *Biomater. Res.* 18 (2014) 8.
- [11] N. Cui, J. Qian, T. Liu, N. Zhao, H. Wang, Hyaluronic acid hydrogel scaffolds with a triple degradation behavior for bone tissue engineering, *Carbohydr. Polym.* 126 (2015) 192–198.
- [12] C. Mahapatra, G.Z. Jin, H.W. Kim, Alginate-hyaluronic acid-collagen composite hydrogel favorable for the culture of chondrocytes and their phenotype maintenance, *Tissue Eng. Regen. Med.* 13 (2016) 538–546.
- [13] F. Chen, Y. Ni, B. Liu, T. Zhou, C. Yu, Y. Su, X. Zhu, X. Yu, Y. Zhou, Self-crosslinking and injectable hyaluronic acid/RGD-functionalized pectin hydrogel for cartilage tissue engineering, *Carbohydr. Polym.* 166 (2017) 31–44.
- [14] Y. Jiao, X. Pang, G. Zhai, Advances in hyaluronic acid-based drug delivery systems, *Curr. Drug Targets* 17 (2016) 720–730.
- [15] C. Fiorica, F.S. Palumbo, G. Pitarresi, F. Bongiovi, G. Giammona, Hyaluronic acid and beta cyclodextrins films for the release of corneal epithelial cells and dexamethasone, *Carbohydr. Polym.* 166 (2017) 281–290.
- [16] G. Wang, S. Gao, R. Tian, J. Miller-Kleinhenz, Z. Qin, T. Liu, L. Li, F. Zhang, Q. Ma, L. Zhu, Theranostic hyaluronic acid-iron micellar nanoparticles for magnetic-field-enhanced in vivo cancer chemotherapy, *ChemMedChem* 13 (2018) 78–86.
- [17] V. Ricci, D. Zonari, S. Cannito, A. Marengo, M.T. Scupoli, M. Malatesta, F. Carton, F. Boschi, G. Berlier, S. Arpico, Hyaluronated mesoporous silica nanoparticles for active targeting: influence of conjugation method and hyaluronic acid molecular weight on the nanovector properties, *J. Colloid Interface Sci.* 516 (2018) 484–497.
- [18] I. Fernandez-Pineiro, A. Pensado, I. Badiola, A. Sanchez, Development and characterization of chondroitin sulfate- and hyaluronic acid-incorporated sorbitan ester nanoparticles as gene delivery systems, *Eur. J. Pharm. Biopharm.* 125 (2018) 85–94.
- [19] L. Tarusha, S. Paoletti, A. Travan, E. Marsich, Alginate membranes loaded with hyaluronic acid and silver nanoparticles to foster tissue healing and to control bacterial contamination of non-healing wounds, *Journal of materials science, J. Mater. Sci. Mater. Med.* 29 (2018) 22.
- [20] S. Vignesh, A. Sivashanmugam, A. Mohandas, R. Janarthanan, S. Iyer, S.V. Nair, R. Jayakumar, Injectable deferoxamine nanoparticles loaded chitosan-hyaluronic acid coacervate hydrogel for therapeutic angiogenesis, *Colloid Surf. B* 161 (2018) 129–138.
- [21] A.M. Rosales, C.B. Rodell, M.H. Chen, M.G. Morrow, K.S. Anseth, J.A. Burdick, Reversible control of network properties in azobenzene-containing hyaluronic acid-based hydrogels, *Bioconjugate Chem.* 29 (4) (2018) 905–913.
- [22] R.E. Thompson, J. Pardieck, L. Smith, P. Kenny, L. Crawford, M. Shoichet, S. Sakiyama-Elbert, Effect of hyaluronic acid hydrogels containing astrocyte-derived extracellular matrix and/or V2a interneurons on histologic outcomes following spinal cord injury, *Biomaterials* 162 (2018) 208–223.
- [23] J. Lou, R. Stowers, S. Nam, Y. Xia, O. Chaudhuri, Stress relaxing hyaluronic acid-collagen hydrogels promote cell spreading, fiber remodeling, and focal adhesion formation in 3D cell culture, *Biomaterials* 154 (2018) 213–222.
- [24] S. van Uden, J. Silva-Correia, J.M. Oliveira, R.L. Reis, Current strategies for treatment of intervertebral disc degeneration: substitution and regeneration possibilities, *Biomater. Res.* 21 (2017) 22.
- [25] Z. Fan, Z. Xu, H. Niu, N. Gao, Y. Guan, C. Li, Y. Dang, X. Cui, X.L. Liu, Y. Duan, H. Li, X. Zhou, P.H. Lin, J. Ma, J. Guan, An injectable oxygen release system to augment cell survival and promote cardiac repair following myocardial infarction, *Sci. Rep.* 8 (2018) 1371.
- [26] Q. Zhu, X. Li, Z. Fan, Y. Xu, H. Niu, C. Li, Y. Dang, Z. Huang, Y. Wang, J. Guan, Biomimetic polyurethane/TiO₂ nanocomposite scaffolds capable of promoting biomineralization and mesenchymal stem cell proliferation, *Mater. Sci. Eng. C, Mater. Biol. Appl.* 85 (2018) 79–87.
- [27] Z. Fan, M. Fu, Z. Xu, B. Zhang, Z. Li, H. Li, X. Zhou, X. Liu, Y. Duan, P.H. Lin, P. Duann, X. Xie, J. Ma, Z. Liu, J. Guan, Sustained release of a peptide-based matrix metalloproteinase-2 inhibitor to attenuate adverse cardiac remodeling and improve cardiac function following myocardial infarction, *Biomacromolecules* 18 (2017) 2820–2829.
- [28] Y. Xu, M. Fu, Z. Li, Z. Fan, X. Li, Y. Liu, P.M. Anderson, X. Xie, Z. Liu, J. Guan, A pro-survival and proangiogenic stem cell delivery system to promote ischemic limb regeneration, *Acta Biomater.* 31 (2016) 99–113.
- [29] M.A. Velasco, C.A. Narvaez-Tovar, D.A. Garzon-Alvarado, Design, materials, and mechanobiology of biodegradable scaffolds for bone tissue engineering, *BioMed. Res. Int.* 2015 (2015) 729076.
- [30] P. Bulpitt, D. Aeschlimann, New strategy for chemical modification of hyaluronic acid: preparation of functionalized derivatives and their use in the formation of novel biocompatible hydrogels, *J. Biomed. Mater. Res.* 47 (1999) 152–169.
- [31] Y. Luo, K.R. Kirker, G.D. Prestwich, Cross-linked hyaluronic acid hydrogel films: new biomaterials for drug delivery, *J. Controlled Release* 69 (2000) 169–184.
- [32] X.Z. Shu, Y. Liu, Y. Luo, M.C. Roberts, G.D. Prestwich, Disulfide cross-linked hyaluronan hydrogels, *Biomacromolecules* 3 (2002) 1304–1311.
- [33] J. Baier Leach, K.A. Bivens, C.W. Patrick Jr., C.E. Schmidt, Photocrosslinked hyaluronic acid hydrogels: natural, biodegradable tissue engineering scaffolds, *Biotechnol. Bioeng.* 82 (2003) 578–589.
- [34] Y.D. Park, N. Tirelli, J.A. Hubbell, Photopolymerized hyaluronic acid-based hydrogels and interpenetrating networks, *Biomaterials* 24 (2003) 893–900.
- [35] X. Zheng Shu, Y. Liu, F.S. Palumbo, Y. Luo, G.D. Prestwich, In situ crosslinkable hyaluronan hydrogels for tissue engineering, *Biomaterials* 25 (2004) 1339–1348.
- [36] D. Das, S. Pal, Modified biopolymer-dextrin based crosslinked hydrogels: application in controlled drug delivery, *RSC Adv.* 5 (2015) 25014–25050.
- [37] I. Noshadi, S. Hong, K.E. Sullivan, E.S. Sani, R. Portillo-Lara, A. Tamayol, S.R. Shin, A.E. Gao, W.L. Stoppel, L.D. Black, A. Khademhosseini, N. Annabi, In vitro and in vivo analysis of visible light crosslinkable gelatin methacryloyl (GelMA) hydrogels, *Biomater. Sci.-UK* 5 (2017) 2093–2105.
- [38] P. Gupta, M. Adhikary J.C, M.M. Kumar, N. Bhardwaj, B.B. Mandal, Biomimetic, osteoconductive non-mulberry silk fiber reinforced tricomposite scaffolds for bone tissue engineering, *ACS Appl. Mater. Interfaces* 8 (2016) 30797–30810.
- [39] M. Ghosh, M. Halperin-Sternfeld, I. Grigoriants, J. Lee, K.T. Nam, L. Adler-Abramovich, Arginine-presenting peptide hydrogels decorated with hydroxyapatite as biomimetic scaffolds for bone regeneration, *Biomacromolecules* 18 (2017) 3541–3550.
- [40] A. Munoz-Bonilla, O. Leon, M.L. Cerrada, J. Rodriguez-Hernandez, M. Sanchez-Chaves, M. Fernandez-Garcia, Chemical modification of block copolymers based on 2-hydroxyethyl acrylate to obtain amphiphilic glycopolymers, *Eur. Polym. J.* 62 (2015) 167–178.
- [41] P.I. Siafaka, A.P. Zisi, M.K. Exindari, I.D. Karantas, D.N. Bikiaris, Porous dressings of modified chitosan with poly(2-hydroxyethyl acrylate) for topical wound delivery of levofloxacin, *Carbohydr. Polym.* 143 (2016) 90–99.
- [42] T.Y. Zhao, D.L. Sellers, Y.L. Cheng, P.J. Horner, S.H. Pun, Tunable, injectable hydrogels based on peptide-cross-linked cyclized polymer nanoparticles for neural progenitor cell delivery, *Biomacromolecules* 18 (2017) 2723–2731.
- [43] H.J. Lee, A. Sen, S. Bae, J.S. Lee, K. Webb, Poly(ethylene glycol) diacrylate/hyaluronic acid semi-interpenetrating network compositions for 3-D cell spreading and migration, *Acta Biomater.* 14 (2015) 43–52.
- [44] Y. Jin, J. Yamanaka, S. Sato, I. Miyata, C. Yomota, M. Yonese, Recyclable characteristics of hyaluronate-polyhydroxyethyl acrylate blend hydrogel for controlled releases, *J. Controlled Release* 73 (2001) 173–181.
- [45] M. Inukai, Y. Jin, C. Yomota, M. Yonese, Preparation and characterization of hyaluronate-hydroxyethyl acrylate blend hydrogel for controlled release device, *Chem. Pharm. Bull.* 48 (2000) 850–854.
- [46] R.K. Bruick, S.L. McKnight, A conserved family of prolyl-4-hydroxylases that modify HIF, *Science* 294 (2001) 1337–1340.
- [47] M. Ivan, K. Kondo, H. Yang, W. Kim, J. Valiando, M. Ohh, A. Salic, J.M. Asara, W.S. Lane, W.G. Kaelin, Jr., HIF1 α targeted for VHL-mediated destruction by proline hydroxylation: implications for O₂ sensing, *Science* 292 (2001) 464–468.
- [48] I. Chopra, M. Roberts, Tetracycline antibiotics: mode of action, applications, molecular biology, and epidemiology of bacterial resistance, *Microbiol. Mol. Biol. Rev. MMBR* 65 (2001) 232–260 (second page, table of contents).
- [49] K. Zhang, S. Yan, G. Li, L. Cui, J. Yin, In-situ birth of MSCs multicellular spheroids in poly(L-glutamic acid)/chitosan scaffold for hyaline-like cartilage regeneration, *Biomaterials* 71 (2015) 24–34.
- [50] D. Das, S. Zhang, I. Noh, Synthesis and characterizations of alginate-alpha-tricalcium phosphate microparticle hybrid film with flexibility and high mechanical property as a biomaterial, *Biomed. Mater.* 13 (2018) 025008.
- [51] D. Das, S. Bang, S.M. Zhang, I. Noh, Bioactive molecules release and cellular responses of alginate-tricalcium phosphate particles hybrid Gel, *Nanomaterials* 7 (2017).
- [52] D. Das, P. Ghosh, A. Ghosh, C. Haldar, S. Dhara, A.B. Panda, S. Pal, Stimulus-responsive biodegradable, biocompatible, covalently cross-linked hydrogel based on dextrin and poly(N-isopropylacrylamide) for in vitro/in vivo controlled drug release, *ACS Appl. Mater. Interfaces* 7 (2015) 14338–14351.
- [53] N.A. Peppas, J.J. Sahlin, A simple equation for the description of solute release .3. Coupling of diffusion and relaxation, *Int. J. Pharm.* 57 (1989) 169–172.
- [54] A.M. Vasi, M.I. Popa, M. Butnaru, G. Dodi, L. Verestiu, Chemical functionalization of hyaluronic acid for drug delivery applications, *Mater. Sci. Eng. C, Mater. Biol. Appl.* 38 (2014) 177–185.
- [55] J.E. Scott, F. Heatley, W.E. Hull, Secondary structure of hyaluronate in solution – a H-1-Nmr investigation at 300 and 500 Mhz in [(H6)-H-2]Dimethyl sulfoxide solution, *Biochem. J.* 220 (1984) 197–205.
- [56] S. Bang, D. Das, J. Yu, I. Noh, Evaluation of MC3T3Cells proliferation and drug release study from sodium hyaluronate-1, 4-butanediol diglycidyl ether patterned gel, *Nanomaterials* 7 (2017).
- [57] K. Wang, A. Bruce, R. Mezan, A. Kadiyala, L. Wang, J. Dawson, Y. Rojanasakul, Y. Yang, Nanotopographical modulation of cell function through nuclear deformation, *ACS Appl. Mater. Interfaces* 8 (2016) 5082–5092.
- [58] L. Song, K. Wang, Y. Li, Y. Yang, Nanotopography promoted neuronal differentiation of human induced pluripotent stem cells, *Colloids Surf. B Biointerfaces* 148

- (2016) 49–58.
- [59] Y. Yang, K. Wang, X. Gu, K.W. Leong, Biophysical regulation of cell behavior-cross talk between substrate stiffness and nanotopography, *Engineering* 3 (2017) 36–54.
- [60] J. Zhang, J. Guan, X. Qi, H. Ding, H. Yuan, Z. Xie, C. Chen, X. Li, C. Zhang, Y. Huang, Dimethylalloylglycine promotes the angiogenic activity of mesenchymal stem cells derived from iPSCs via activation of the PI3 K/Akt pathway for bone regeneration, *Int. J. Biol. Sci.* 12 (2016) 639–652.
- [61] A.N. Sapadin, R. Fleischmajer, Tetracyclines: nonantibiotic properties and their clinical implications, *J. Am. Acad. Dermatol.* 54 (2006) 258–265.
- [62] C. Maderuelo, A. Zarzuelo, J.M. Lanao, Critical factors in the release of drugs from sustained release hydrophilic matrices, *J. Controlled Release* 154 (2011) 2–19.
- [63] R.P. Batycky, J. Hanes, R. Langer, D.A. Edwards, A theoretical model of erosion and macromolecular drug release from biodegrading microspheres, *J. Pharm. Sci.* 86 (1997) 1464–1477.
- [64] M.M. Talukdar, A. Michoel, P. Rombaut, R. Kinget, Comparative study on xanthan gum and hydroxypropylmethyl cellulose as matrices for controlled-release drug delivery .1. Compaction and in vitro drug release behaviour, *Int. J. Pharm.* 129 (1996) 233–241.